RESEARCH ARTICLE | JULY 31 2024

Quantifying carrier density in monolayer MoS$_2$ by optical spectroscopy ⒺⓅ

Special Collection: Festschrift in honor of Louis E. Brus

Alexis R. Myers ⓘ ; Dana B. Sulas-Kern; Rao Fei ⓘ ; Debjit Ghoshal ⓘ ; M. Alejandra Hermosilla-Palacios ⓘ ;
Jeffrey L. Blackburn ✉ ⓘ
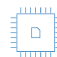
[Check for updates]

[View Online] [Export Citation]

Quantifying carrier density in monolayer MoS$_2$ by optical spectroscopy

View Online   Export Citation   CrossMark

Alexis R. Myers,[1,2] ID   Dana B. Sulas-Kern,[2] Rao Fei,[2,3] ID Debjit Ghoshal,[2] ID
M. Alejandra Hermosilla-Palacios,[2,a)] ID and Jeffrey L. Blackburn[2,b)] ID

AFFILIATIONS

[1] Department of Chemistry, University of Colorado Boulder, Boulder, Colorado 80309, USA

[2] National Renewable Energy Laboratory, Golden, Colorado 80401, USA

[3] Materials Science and Engineering Program, University of Colorado Boulder, Boulder, Colorado 80309, USA

Note: This paper is part of the JCP Festschrift in honor of Louis E. Brus.
a)Electronic Mail: alejandra.hermosillapalacios@nrel.gov
b)Author to whom correspondence should be addressed: jeffrey.blackburn@nrel.gov

ABSTRACT

The successful design and device integration of nanoscale heterointerfaces hinges upon precise manipulation of both ground- and excited-state charge carrier (electron and hole) densities. However, it is particularly challenging to quantify these charge carrier densities in nanoscale materials, leading to uncertainties in the mechanisms of many carrier density-dependent properties and processes. Here, we demonstrate a method that utilizes steady-state and transient absorption spectroscopies to correlate monolayer MoS$_2$ electron density with the easily measured metric of excitonic optical absorption quenching in a variety of mixed-dimensionality s-SWCNT/MoS$_2$ heterostructures. By employing a 2D phase-space filling model, the resulting correlation elucidates the relationship between charge density, local dielectric environment, and concomitant excitonic properties. The phase-space filling model is also able to describe existing trends from the literature on transistor-based measurements on MoS$_2$, WS$_2$, and MoSe$_2$ monolayers that were not previously compared to a physical model, providing additional support for our method and results. The findings provide a pathway to the community for estimating both ground- and excited-state carrier densities in a wide range of TMDC-based systems.

I. INTRODUCTION

Two-dimensional (2D) layered semiconductors, such as transition metal dichalcogenides (TMDCs), have been studied intensively for over forty years.[1,2] The successful isolation and growth of monolayer TMDCs in the past ten years ushered in the development and studies of TMDC heterostructures for use in optoelectronic, catalytic, and quantum information processing applications,[3–7] due to the emergence of a direct bandgap and other beneficial properties, such as spin–valley locking.[8,9] Despite these advances, several fundamental knowledge gaps remain for monolayer TMDCs and their heterostructures. In general, the optimization of semiconductor heterostructures depends on the knowledge of both ground- and excited-state carrier densities, which dictate the steady-state and transient properties of optoelectronic devices. Quantitative

assessment of charge carrier concentrations can be challenging for monolayer TMDCs, since traditional methods rely upon an accurate knowledge of properties, such as dielectric constant,[10] effective mass or mobility,[11] and device capacitance,[12] all of which can be challenging to measure and are impacted in uncertain ways by the local environment.[13]

Several decades ago, the III–V community developed a powerful, but simple, method based on optical absorption spectroscopy to quantify carrier densities and carrier-density dependent properties in GaAs quantum wells, an early 2D excitonic material. This model, based on the phase space filling effect, related the carrier density in the two-dimensional layer to the resulting quenching of the strong excitonic optical transitions.[14,15] Recent studies have also applied similar models to semiconducting single-walled carbon nanotubes (s-SWCNTs) as a model one-dimensional (1D) excitonic

semiconductor.[16,17] A key to this phase-space filling model is the knowledge, or estimate, of the exciton size, since that determines the fraction of exciton oscillator strength that is quenched by a particular charge carrier density. In turn, this exciton size is influenced by the reduced exciton mass and the dielectric constant experienced by the exciton. Applying such a model to monolayer TMDCs is an attractive possibility but is made challenging by the large experimental and theoretical variations in reported dielectric constants (that can depend on sample substrate, thickness, and growth methods)[10,18,19] and excitonic constants.[11,20,21]

Applying a phase-space filling model to TMDCs requires a means to systematically vary the monolayer carrier density, a series of experimentally measured absorption or reflection spectra at each carrier density, and a reliable way to quantify the carrier density for each spectrum. Carrier density can be modulated by the gate-voltage in a transistor, via molecular or substitutional ground-state doping, or via dynamic processes, such as photoinduced charge transfer. Some transistor-based studies have reported trends for the dependence of exciton oscillator strength, measured by reflectance, on carrier density in MoS_2,[22] WS_2,[23] and $MoSe_2$[24] monolayers, but these studies have not simulated those results with a physically relevant model, such as a phase-space filling dependence. The carrier density in these studies is extracted by considering the gate oxide capacitance and the difference between the applied gate voltage and the gate voltage associated with the charge neutrality point. However, the carrier density is dictated by the total gate capacitance, equal to the sum of the gate oxide capacitance and the channel quantum capacitance. It has been pointed out that the monolayer TMDC quantum capacitance can dominate the total capacitance, leading to errors in extracting carrier density by using the gate oxide capacitance alone.[12] With these considerations in mind, the need

remains for a rigorous analysis aimed at quantifying carrier density in monolayer TMDCs by optical spectroscopy.

In this study, we quantify carrier density in monolayer MoS_2 by using an "internal standard," in this case a one-dimensional (1D) electron donor in a series of mixed-dimensionality (1D/2D) donor/acceptor heterostructures (see Fig. 1),[25,26] and employ a 2D phase-space filling model to simulate the dependence of MoS_2 exciton bleach on carrier density. This study expands upon the concept recently introduced by Sulas-Kern *et al.*,[25] where the optical cross section for charges in a semiconducting single-walled carbon nanotube (s-SWCNT) thin film was used to quantify charge separation quantum yield in a photoexcited s-SWCNT/MoS_2 heterostructure. That proof-of-concept demonstration was limited in that it only utilized a single value of excited-state charge yield and only a single study at the time[27] had estimated a charge carrier (hole) cross section in the highly enriched (6,5) s-SWCNTs used as electron donors. Since that study, Eckstein *et al.* utilized spectro-electrochemistry and a 1D phase-space filling model to quantify hole density in (6,5) s-SWCNTs,[16] and we have performed additional studies on mixed-dimensionality s-SWCNT/MoS_2 heterostructures.[26,28] Furthermore, an experimental diamagnetic shift study[20] that came out shortly after Sulas-Kern *et al.*[25] provided a rigorously determined reduced exciton mass for high-quality MoS_2 that allows us to better constrain the 2D phase-space filling model.

With two independent estimates now available for (6,5) s-SWCNTs,[16,27] we use this s-SWCNT "internal standard" to rigorously correlate MoS_2 electron yield and exciton quenching in a variety of photoexcited s-SWCNT/MoS_2 heterostructures. This method allows us to greatly constrain the potential range of physical properties used in a 2D phase-space filling model for the MoS_2 component of the heterostructure. The resulting correlation between
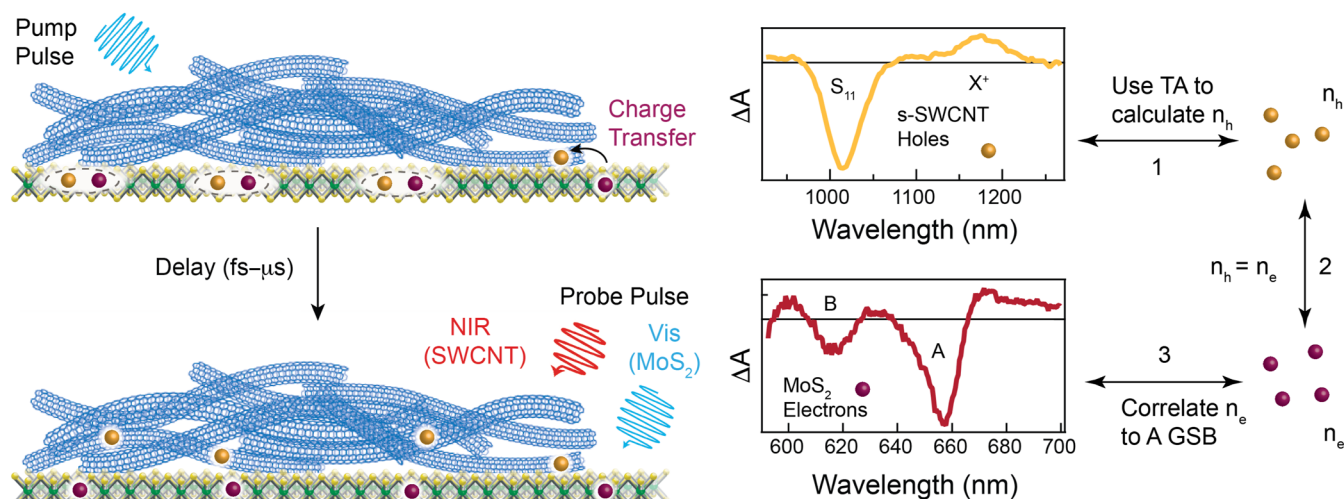
FIG. 1. Schematic of the method employed here to quantify the impact of charge carrier (electron) density on MoS_2 A exciton quenching (ground-state bleach or GSB). Pump–probe transient absorbance spectroscopy follows the photoinduced charge transfer in a photoexcited bilayer (example shown) or trilayer containing MoS_2 and a (6,5) s-SWCNT thin film (the internal standard). Following photoinduced charge transfer, the following steps are used to quantify this dependence: (1) The known absorption cross sections of (6,5) s-SWCNT charge-related TA features are used to calculate the s-SWCNT hole density (n_h). (2) Based on charge balance, the electron density in MoS_2 (n_e) is equivalent to n_h. (3) The GSB magnitude in MoS_2 can then be correlated directly to n_e.

electron density and MoS_2 carrier-induced exciton quenching can be used by the community to estimate both ground- and excited-state carrier densities in a wide range of MoS_2-based systems, such as photoexcited heterostructures, (photo)transistors, and redox-doped or electrochemically doped monolayers. Our results also provide well-constrained ranges for fundamental MoS_2 monolayer properties, such as exciton size and dielectric constant.

II. RESULTS AND DISCUSSION

Figure 2(a) displays the representative steady-state absorption spectra of the mixed-dimensionality heterostructures probed in this study. Both types of heterostructures employ highly enriched (6,5) s-SWCNTs as a photoexcited electron donor and MoS_2 as a photoexcited electron acceptor. The first heterostructure is a s-SWCNT/MoS_2 bilayer,[25,26] and the second is a WSe_2/s-SWCNT/MoS_2 trilayer that forms a charge transfer cascade.[28] Strong excitonic absorption features related to both the (6,5) s-SWCNTs and TMDC components are labeled in the figure.

Our study employs femtosecond pump–probe transient absorption (TA) spectroscopy to follow photoinduced charge transfer in these heterostructures. Specific excitonic and charge-related features in TMDCs and SWCNTs have revealed that SWCNTs aid in the spatial separation of charges in these TMDC–SWCNT based heterostructures, resulting in exceptionally long (>μs) charge-separated lifetimes.[25,26,28] In this study, we use the magnitude of these transient spectral features following the completion of photoinduced charge transfer to quantify charge carrier quantum yield and ultimately to develop the phase-space filling "calibration curve" for monolayer MoS_2 (Fig. 1). A judicious choice of the pump photon energy is employed to predominantly excite the s-SWCNT or TMDC components of the heterostructures.

Figure 2(b) displays the TA spectra, taken at 5 ps pump–probe delay, for a representative s-SWCNT thin film, a s-SWCNT/MoS_2

bilayer, and a WSe_2/s-SWCNT/MoS_2 trilayer. TA features in the visible range can be assigned to the ground-state bleach (GSB) of the MoS_2 and WSe_2 excitonic transitions and the GSB of the (6,5) S_{22} excitonic transition. Features in the near-infrared (NIR) range can be assigned to the (6,5) S_{11} GSB and the trion induced absorption (IA), a feature that is only present when separated charge carriers (electrons or holes) are present on the s-SWCNTs. These distinct spectral features can be used to quantitatively track the temporal evolution of exciton dissociation, charge diffusion, and charge recombination in the mixed-dimensionality heterostructures.[25,26,28]

The charge transfer quantum yield (ϕ_{CT}) is defined as the number of separated charges (i.e., holes and electrons in separate materials) produced per photogenerated exciton. We estimate charge transfer yields for our type II heterostructures using two separate methods that utilize (1) an empirically determined trion absorption cross section that uses a heuristic model of the dependence of exciton bleaching on redox-doping induced carrier density[27] and (2) a correlation between electrochemically modulated charge density and exciton bleach that utilizes a 1D phase-space filling model.[16] Each method utilizes a similar overall methodology of tracking the dependence of the ground-state bleach (GSB) and trion IA on carrier density, but they utilize different frameworks for predicting the impact of the SWCNT density of states on this dependence. Until now, the two studies have not been compared to determine how well-matched their values may be for estimating SWCNT (or SWCNT heterostructure) carrier densities.

For each method described above, we first use singular value decomposition, accompanied by the associated kinetic rate equations, to simulate the full two-dimensional array of time-dependent TA spectra.[25,26,28] These simulations produce concentration trajectories for the relevant species (e.g., excitons in photoexcited s-SWCNTs; charges in s-SWCNTs and TMDCs following exciton dissociation) evolving in time following the pump pulse. This method allows us to isolate and quantify charge-related s-SWCNT and MoS_2 TA features.
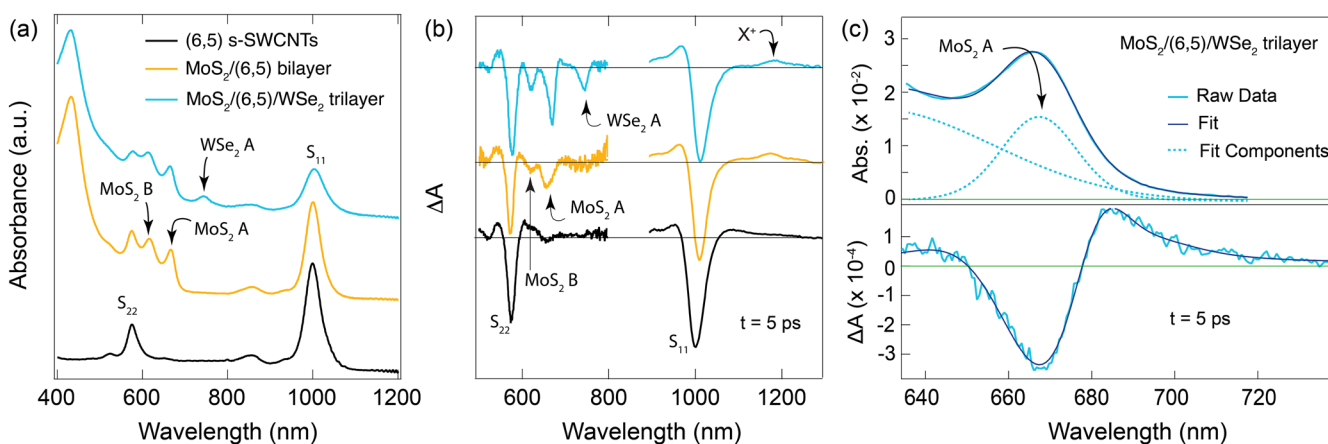
FIG. 2. (a) Steady-state and (b) transient absorbance spectra of a neat (6,5) s-SWCNT (black), a s-SWCNT/MoS_2 bilayer (orange), and a WSe_2/s-SWCNT/MoS_2 trilayer (blue). The labels identify salient excitonic absorption features for the s-SWCNTs (S_{11} and S_{22}) and TMDCs (A and B excitons), along with the s-SWCNT trion induced absorbance (X^+). (c) Exemplary spectral fits (Voigt line shapes) applied to the MoS_2 steady-state (top panel) and transient (bottom panel) absorbance spectra to extract A_0 and ΔA, respectively. These values are used to quantify the extent of exciton bleach ($\Delta A/A_0$) for a particular photoinduced carrier density.

Within the model proposed by Dowgiallo et al. (method 1 from above; supplementary material, Sec. 3.1), the intensity of the trion induced absorption can be normalized to the ground state S_{11} absorption ($OD_{X(+/-)}/OD_{S_{11}}$) to calculate the s-SWCNT carrier density. The trion optical density used to calculate s-SWCNT hole density derives from the TA spectrum associated with the concentration profiles where a given interfacial charge transfer reaction has reached completion (Figs. S1–S2). The s-SWCNT charge carrier concentration is then given by

$$\frac{OD(X^+)}{OD(S_{11})} = 0.0674 - 0.0676e^{-21.5N_{h/e}}, \quad (1)$$

where $N_{h/e}$ is the hole or electron density/nm of tube length.

The second method (supplementary material, Sec. 3.2) relies on the 1D phase-space filling model developed by Eckstein et al. to correlate (6,5) s-SWCNT charge density to fractional exciton bleach.[16] The fractional exciton bleach is defined as

$$\frac{A_{S_{11}} GSB}{A_{S_{11}} abs}, \quad (2)$$

where $A_{S_{11}}$ GSB and $A_{S_{11}}$ abs are the area under the curve for the S_{11} ground state bleach from the TA spectrum and S_{11} ground state absorption, respectively (see Figs. S3–S5 of the supplementary material).

Both these methods allow us to extract the s-SWCNT carrier density in units of nm^{-1}. Since we are ultimately concerned with deriving an areal carrier density within the MoS$_2$ layer, we convert this s-SWCNT carrier density to units of cm^{-2} by using the absorbance of the s-SWCNT film, the empirical absorbance coefficient for (6,5) s-SWCNTs, and the number of carbon atoms per nm in a (6,5) s-SWCNT (see Sec. 2 of the supplementary material). For s-SWCNT/MoS$_2$ bilayers, the calculated s-SWCNT hole density equals the MoS$_2$ electron density, since there is only one exciton dissociation interface and one exciton splits into one electron and one hole. The WSe$_2$/s-SWCNT/MoS$_2$ trilayer is more complex because excitons can be dissociated at two separate interfaces to produce electrons in MoS$_2$ and holes in WSe$_2$ [see Fig. 2(c) of the supplementary material]. Thus, the concentration trajectories for each species must be used to calculate the fraction of s-SWCNT holes produced by exciton dissociation at the s-SWCNT/MoS$_2$ interface and the fraction of s-SWCNT electrons produced by exciton dissociation at the s-SWCNT/WSe$_2$ interface (Figs. S1 and S2). The MoS$_2$ electron density is then equivalent to the calculated s-SWCNT hole density.

Table I compares the s-SWCNT and MoS$_2$ carrier densities extracted from each of the methods described above. The two methods agree reasonably well, with percent difference ranging from ~3% to 37% (excluding the bilayer excited at 532 nm). The good agreement between the methods proposed by Dowgiallo et al.[27] and Eckstein et al.[16] suggest that each method is viable for estimating s-SWCNT ground- or excited-state carrier density and provides additional confidence in the extracted MoS$_2$ carrier densities used in the following calibration curve.

Turning to the MoS$_2$ components of the heterostructures, we can now correlate the extracted MoS$_2$ carrier densities to the associated MoS$_2$ A exciton bleach values. To produce the phase-space filling correlation we ultimately desire,[14,15] we must calculate the extent of MoS$_2$ exciton bleaching for a given photoinduced carrier density. This calculation is achieved by performing a spectral deconvolution of the steady-state and transient absorbance spectra in the region of the MoS$_2$ A exciton, as shown in Fig. 2(c) (see also Figs. 6 and 7 of the supplementary material). All steady-state absorbance features have a positive sign, so once the peak for the A exciton is extracted via spectral deconvolution, the area of this peak is used for the original A exciton absorbance (A_0). The TA spectrum can be more complex, since spectral shifts and transfer of oscillator strength to trion absorption can induce positive features in addition to the negative GSB.[29] As such, the spectrum is fit to a combination of both negative and positive peaks and the total area of the ground-state bleach (GSB) is taken as the summation of the areas (absolute values) of each of these peaks.[29]

The phase-space filling effect dictates that electrons in the MoS$_2$ conduction band remove states that contribute oscillator strength to

TABLE I. Carrier density calculated from both methods discussed above for the MoS$_2$/SWCNT/WSe$_2$ trilayer and multiple MoS$_2$/SWCNT bilayer samples and excitation wavelength corresponding to either hole transfer (HT) or electron transfer (ET) and their relative difference.

Sample	λ_{exc} (nm)	Fluence (μJ/cm^2)	Rxn	MoS$_2$ A GSB[a]	MoS$_2$ n_e[b] (cm^{-2})	MoS$_2$ n_e[c] (cm^{-2})	%Diff[d]
Bilayer 1	1000	50.0	ET	0.049	1.05×10^{12}	7.19×10^{11}	37
Bilayer 1	440	4.60	HT	0.039	8.34×10^{11}	5.81×10^{11}	36
Bilayer 2	1000	1.06	ET	0.0076	3.41×10^{11}	3.53×10^{11}	3.6
Bilayer 2	440	3.35	HT	0.022	6.19×10^{11}	8.68×10^{11}	34
Bilayer 3	1000	1.50	ET	0.000 97	4.10×10^{11}	4.84×10^{11}	16
Bilayer 3	532	50.0	HT	0.1132	2.14×10^{12}	1.23×10^{12}	54
Trilayer	1000	7.41	ET	0.0032	7.43×10^{10}	1.05×10^{11}	34

[a] Percentage bleach, i.e., $\Delta A/A_0$, where $f(N)/f(0) = 1 - (\Delta A/A_0)$.
[b] Method of Dowgiallo et al.[27] used to calculate s-SWCNT n_h.
[c] Method of Eckstein et al.[16] used to calculate s-SWCNT n_h.
[d] Difference = $[n_e^\# - n_e^@]/[(n_e^\# + n_e^@)/2] \times 100$.

14 August 2024 15:20:19

excitonic transitions, thus decreasing oscillator strength (f).[14,15] A known solution to the Schrödinger equation can be used when the exciton is represented as an isolated state in an ideal quantum well, where the functional form of the wavefunction is minimally affected by carrier density, but the carriers perturb the exciton size and binding energy via screening (supplementary material, Sec. 4 and Fig. S8).[14] Here, the magnitude of exciton bleaching can be related to physical properties in the TMDC, such as the dielectric constant (ε) and reduced exciton mass (μ), both of which impact the effective Bohr radius (a_0),

$$\frac{f(N)}{f(0)} = \frac{1}{1 + N/N_c}, \quad (3)$$

where N is the density of charge carriers and $N_c = 2/\pi a_0^2$ is the critical carrier density at which 50% of the oscillator strength is quenched. N_c in turn depends on the exciton size,

$$a_0 = \frac{\varepsilon \hbar^2}{e^2 \mu}, \quad (4)$$

where $\hbar$ is the reduced Planck constant and e is the elementary charge. In Fig. 3, we use a reduced exciton mass (μ) of $0.275 m_e$ for MoS$_2$ (where m_e is the electron mass), based on the recent study by Goryca et al.[20] With a well-constrained empirical value for μ, the exciton size and corresponding dependence of exciton bleach on carrier density depend primarily on the local dielectric environment, so Fig. 3 displays multiple plots with dielectric constants ranging from 4 to 16.5.[3,25]

The experimental data fall within a dielectric constant range of 5.5–12.5, with a best fit of ~8.0 for the apparent local dielectric constant. To rationalize this range, we consider the average dielectric constant, $\varepsilon_{avg} = 1/2 (\varepsilon_{top} + \varepsilon_{bottom})$, of the materials surrounding the MoS$_2$ layer. While this approach is commonly applied to understand Coulomb screening, phase space filling, and bandgap

renormalization in monolayer TMDCs, some studies use the static dielectric constant of the adjacent materials,[30] while other studies utilize the high-frequency dielectric constants.[20,31] If we first consider the static dielectric constants of sapphire [$\varepsilon_0 = 9$–9.4 (in-plane), $\varepsilon_0 = 11.6$–11.8 (out-of-plane), and $\varepsilon_{avg} = 10.5$][32,33] and SWCNTs ($\varepsilon_0 = 4.0$),[34–36] we arrive at $\varepsilon_{avg} = 7.3$. Turning to the high-frequency dielectric constants, using $\varepsilon_0 = 4.0$ for the s-SWCNT film and $\varepsilon_\infty = 3.05$ for sapphire[33] leads to $\varepsilon_{avg} = 3.5$. While there are insufficient reports of the high-frequency dielectric constant of highly enriched (near-monochiral) s-SWCNTs in the literature, a recent report suggests that the dielectric function is relatively flat in the far-infrared regime.[37]

At first glance, this analysis suggests that the use of static dielectric constants might be most appropriate for describing phase-space filling in these photoexcited heterojunctions. To test this, we studied s-SWCNT/MoS$_2$ bilayers prepared on MgF$_2$ ($\varepsilon_0 = 5.2$, $\varepsilon_\infty = 1.7$, square data points in Fig. 3)[32,38] instead of sapphire. The average dielectric environment between MgF$_2$ and s-SWCNTs would be ~$\varepsilon_{avg} = 4.1$ and $\varepsilon_{avg} = 2.4$, using static and high-frequency dielectric constants, respectively. The MgF$_2$ results all fall near the $\varepsilon = 5.5$ fit line, in reasonable agreement with the average static dielectric constants, but incommensurate with the high-frequency dielectric constants. As such, we tentatively conclude that phase-space filling in these photoexcited monolayer MoS$_2$ heterostructures is best described by considering the static dielectric constants of the surrounding materials.

To put our results into context with the existing literature, we have also plotted the results of several studies that correlated exciton quenching with the carrier density of monolayer TMDC transistor channels. As shown in Fig. 3(b), the bounds of the phase-space filling model employed in our study do a good job of describing existing monolayer MoS$_2$ transistor-based measurements.[22] This comparison provides additional confidence in our results and may also suggest that using the gate oxide capacitance to extract carrier density is a reasonable approximation for the transistors studied by
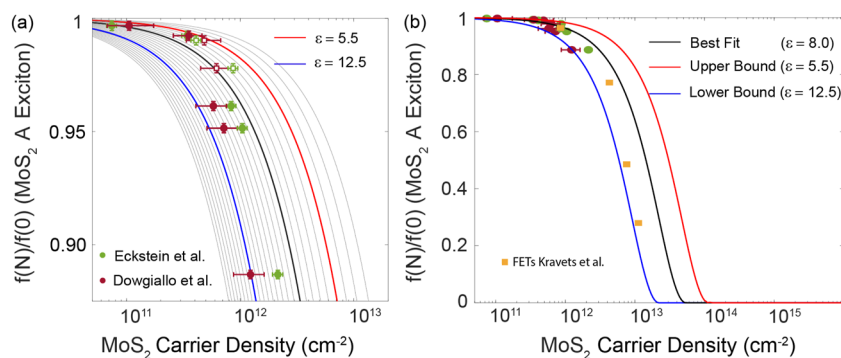
FIG. 3. Charge density (N) dependence of the exciton oscillator strength (f) from the phase-space filling model, plotted for varying dielectric constants (ε) produced in MoS$_2$ by exciton dissociation at the MoS$_2$/SWCNT interface in either bilayers or trilayers. Bilayers prepared on MgF$_2$ are open squares, and all other samples are on sapphire and correspond to filled circles. Going from right to left, the dielectric constant varies from 4 to 16.5 in steps of 0.5. The red and green points refer to data extracted by using the methods of Eckstein et al. and Dowgiallo et al., respectively, to calculate the photoinduced s-SWCNT carrier density (see Table I). Additional details of the constants used in the phase-space filling model are given in the text. Panel (a) provides a zoomed in view of the dependence focusing on the individual data points, while panel (b) provides the full dependence that can be used by the community for experiments producing any carrier density, associated exciton bleach, and the FETs experimental data points from Kravets and co-workers.[22]

Kravets et al.[22] Similarly, separately derived phase-space filling simulations do a good job of describing the transistor-based trends found for WS$_2$[23] and MoSe$_2$[24] monolayers (Fig. S9).

We can also connect our results to the prevailing literature exploring the carrier density-dependent renormalization of electronic (quasiparticle) bandgap and exciton binding energy in monolayer MoS$_2$. Bandgap renormalization is known to be substantial in doped TMDCs and has been studied extensively for MoS$_2$.[39–41] Since the phase-space filling model depends on the exciton binding energy, we turn to the study of Yao et al. that discriminated between the impacts of injected charge carriers on the electronic bandgap and exciton binding energy.[42] In Fig. S10, we plot the carrier density-dependent change in exciton binding energy, normalized to the original binding energy, for the best-fit and upper/lower bounds of the phase space filling simulation in Fig. 3, along with the same trend found by Yao et al. (green data points). The data from Yao et al.[42] fall nicely within the bounds predicted by our phase-space simulation, providing additional confidence in our results.

Returning to Fig. 3(b), while the data at low carrier densities are most consistent with an apparent local dielectric constant in the range of ~5.5, the data move progressively toward fit lines corresponding to higher apparent dielectric constants (up to ~12.5) as carrier density increases. This trend suggests that, although it appears to capture the expected excitonic transition bleaching by charge carriers quite well, the 2D phase-space filling model may not capture all of the underlying physics at play in monolayer MoS$_2$. Since our spectroscopic data and data from transistor-based measurements both seem to fall off slightly faster than might be predicted by the phase-space filling model, we consider it most likely that the behavior is intrinsic to TMDCs and does not reflect a shortcoming of either type of measurement methods.

The phase-space filling curve elucidated here (with upper/lower bounds) can be used by the community to determine monolayer MoS$_2$ carrier density in a number of different experiments, as long as the samples/devices can be interrogated by transmission or reflection-based optical spectroscopy. These include experiments and devices where steady-state carrier densities are injected into the monolayer via electrostatic [e.g., (photo)transistors][43,44] or electrochemical gating (e.g., ion-gated transistors or spectroelectrochemical cells)[40] or by adsorbed molecular redox dopants,[45] as well as time-resolved experiments where excited-state carrier densities are modulated by dynamic processes, such as photoinduced charge transfer.[3] To recreate the full phase-space filling model shown in Fig. 3, one can use Eqs. (3) and (4) and the most appropriate estimate for the dielectric environment [$\varepsilon_{avg} = 1/2 \, (\varepsilon_{top} + \varepsilon_{bottom})$] of the monolayer sample, to generate the relevant dependence. We suggest the use of the recently derived reduced exciton mass $\mu = 0.275 m_e$[20] and, based on the empirical data shown here, the static dielectric constants of the surrounding materials.

III. CONCLUSION

In this study, we develop a scaling curve that correlates the loss of A exciton oscillator strength in monolayer MoS$_2$ to the 2D carrier density by means of a s-SWCNT internal standard in a series of photoinduced mixed-dimensionality type II heterostructures. The trends in Fig. 3 highlight that determining an appropriate value for the dielectric constant experienced by an exciton in a monolayer MoS$_2$/s-SWCNT system is not trivial. The scaling curve utilizes a phase-space filling model originally developed for 2D quantum wells and incorporates empirically valid values for the physical properties of 2D MoS$_2$ excitons. The consistency between various s-SWCNT/MoS$_2$ samples within the phase-space filling model supports the use of similar carrier density scaling curves proposed recently by Eckstein et al. and Dowgiallo et al., expanding the relatively underdeveloped assessment of charge carrier concentration in monolayer TMDCs. This study also demonstrates that the well-defined charge-associated transient absorption spectral features s-SWCNTs provide a useful guidepost for understanding how to reliably quantify charge transfer quantum yield and the role of dielectric environment on charge separation and recombination when paired with a variety of TMDCs.

SUPPLEMENTARY MATERIAL

The supplementary material contains materials and methods and calculations for N$_{exc}$, charge yield, and the phase-space filling model.

ACKNOWLEDGMENTS

AUTHOR DECLARATIONS

Conflict of Interest

The authors have no conflicts to disclose.

Author Contributions

Alexis R. Myers: Data curation (equal); Formal analysis (equal); Investigation (equal); Methodology (equal); Visualization (equal); Writing – original draft (equal); Writing – review & editing (equal). **Dana B. Sulas-Kern**: Data curation (equal); Investigation (equal); Writing – review & editing (equal). **Rao Fei**: Data curation (equal); Investigation (equal); Writing – review & editing (equal). **Debjit Ghoshal**: Data curation (equal); Formal analysis (equal); Investigation (equal); Writing – review & editing (equal). **M. Alejandra Hermosilla-Palacios**: Conceptualization (equal); Data curation (equal); Formal analysis (equal); Investigation (equal); Methodology (equal); Validation (equal); Visualization (equal); Writing – original draft (equal); Writing – review & editing (equal). **Jeffrey L. Blackburn**: Conceptualization (equal); Data curation (equal); Formal analysis (equal); Funding acquisition (equal); Investigation (equal); Methodology (equal); Project administration (equal);

Resources (equal); Supervision (equal); Validation (equal); Visualization (equal); Writing – original draft (equal); Writing – review & editing (equal).

DATA AVAILABILITY

The data that support the findings of this study are available from the corresponding author upon reasonable request.

REFERENCES

[1] B. A. Parkinson, T. E. Furtak, D. Canfield, K.-K. Kam, and G. Kline, "Evaluation and reduction of efficiency losses at tungsten diselenide photoanodes," Faraday Discuss. Chem. Soc. **70**, 233–245 (1980).

[2] H. Tributsch and J. C. Bennett, "Electrochemistry and photochemistry of MoS₂ layer crystals. I," J. Electroanal. Chem. Interfacial Electrochem. **81**, 97–111 (1977).

[3] D. B. Sulas-Kern, E. M. Miller, and J. L. Blackburn, "Photoinduced charge transfer in transition metal dichalcogenide heterojunctions – towards next generation energy technologies," Energy Environ. Sci. **13**, 2684–2740 (2020).

[4] M. I. B. Utama, A. Dasgupta, R. Ananth, E. A. Weiss, T. J. Marks, and M. C. Hersam, "Mixed-dimensional heterostructures for quantum photonic science and technology," MRS Bull. **48**, 905–913 (2023).

[5] R. Yang, J. Fan, and M. Sun, "Transition metal dichalcogenides (TMDCs) heterostructures: Optoelectric properties," Front. Phys. **17**, 43202 (2022).

[6] T. Sun, H. Zhang, X. Wang, J. Liu, C. Xiao, S. U. Nanayakkara, J. L. Blackburn, M. V. Mirkin, and E. M. Miller, "Nanoscale mapping of hydrogen evolution on metallic and semiconducting MoS₂ nanosheets," Nanoscale Horiz. **4**, 619–624 (2019).

[7] Z. Li, N. H. Attanayake, J. L. Blackburn, and E. M. Miller, "Carbon dioxide and nitrogen reduction reactions using 2D transition metal dichalcogenide (TMDC) and carbide/nitride (MXene) catalysts," Energy Environ. Sci. **14**, 6242–6286 (2021).

[8] K. Wang, K. De Greve, L. A. Jauregui, A. Sushko, A. High, Y. Zhou, G. Scuri, T. Taniguchi, K. Watanabe, M. D. Lukin, H. Park, and P. Kim, "Electrical control of charged carriers and excitons in atomically thin materials," Nat. Nanotechnol. **13**, 128–132 (2018).

[9] R. Krishnan, S. Biswas, Y.-L. Hsueh, H. Ma, R. Rahman, and B. Weber, "Spin-valley locking for in-gap quantum dots in a MoS₂ transistor," Nano Lett. **23**, 6171–6177 (2023).

[10] S.-L. Li, K. Tsukagoshi, E. Orgiu, and P. Samorì, "Charge transport and mobility engineering in two-dimensional transition metal chalcogenide semiconductors," Chem. Soc. Rev. **45**, 118–151 (2016).

[11] A. Thilgam, "Exciton complexes in low dimensional transition metal dichalcogenides," J. Appl. Phys. **116**, 053523 (2014).

[12] N. Ma and D. Jena, "Carrier statistics and quantum capacitance effects on mobility extraction in two-dimensional crystal semiconductor field-effect transistors," 2D Mater. **2**, 015003 (2015).

[13] A. Raja, A. Chaves, J. Yu, G. Arefe, H. M. Hill, A. F. Rigosi, T. C. Berkelbach, P. Nagler, C. Schüller, T. Korn *et al.*, "Coulomb engineering of the bandgap and excitons in two-dimensional materials," Nat. Commun. **8**, 15251 (2017).

[14] D. Huang, J.-I. Chyi, and H. Morkoç, "Carrier effects on the excitonic absorption in GaAs quantum-well structures: Phase-space filling," Phys. Rev. B **42**, 5147–5153 (1990).

[15] A. Cameron, P. Riblet, and A. Miller, "Broadening, screening, and phase space filling in GaAs multiple quantum wells revisted," in *Quantum Electronics and Laser Science Conference* (IEEE, 1996), Vol. 10.

[16] K. H. Eckstein, F. Oberndorfer, M. M. Achsnich, F. Schöppler, and T. Hertel, "Quantifying doping levels in carbon nanotubes by optical spectroscopy," J. Phys. Chem. C **123**, 30001–30006 (2019).

[17] M. A. Hermosilla-Palacios, M. Martinez, E. A. Doud, T. Hertel, A. M. Spokoyny, S. Cambré, W. Wenseleers, Y.-H. Kim, A. J. Ferguson, and J. L. Blackburn, "Carrier density and delocalization signatures in doped carbon nanotubes from quantitative magnetic resonance," Nanoscale Horiz. **9**, 278–284 (2024).

[18] S. Park, N. Mutz, T. Schultz, S. Blumstengel, A. Han, A. Aljarb, L.-J. Li, E. J. List-Kratochvil, P. Amsalem, and N. Koch, "Direct determination of monolayer MoS₂ and WSe₂ exciton binding energies on insulating and metallic substrates," 2D Mater. **5**, 025003 (2018).

[19] A. Laturia, M. L. Van de Put, and W. G. Vandenberghe, "Dielectric properties of hexagonal boron nitride and transition metal dichalcogenides: From monolayer to bulk," npj 2D Mater. Appl. **2**, 6 (2018).

[20] M. Goryca, J. Li, A. Stier, T. Taniguchi, K. Watanabe, E. Courtade, S. Shree, C. Robert, B. Urbaszek, X. Marie, and S. Crooker, "Revealing exciton masses and dielectric properties of monolayer semiconductors with high magnetic fields," Nat. Commun. **10**, 4172 (2019).

[21] S. Latini, K. T. Winther, T. Olsen, and S. Thygesen, "Interlayer excitons and band alignment in MoS₂/hBN/WSe₂ van der Waals heterostructures," Nano Lett. **17**, 938–945 (2017).

[22] V. G. Kravets, F. Wu, G. H. Auton, T. Yu, S. Imaizumi, and A. Grigorenko, "Measurements of electrically tunable refractive index of MoS₂ monolayer and its usage in optical modulators," npj 2D Mater. Appl. **3**, 36 (2019).

[23] Y. Yu, Y. Yu, L. Huang, H. Peng, L. Xiong, and L. Cao, "Giant gating tunability of optical refractive index in transition metal dichalcogenide monolayers," Energy Environ. Sci. **12**, 1648–1656 (2017).

[24] M. Li, S. Biswas, C. Hail, and H. Atwater, "Refractive index modulation in monolayer molybdenum diselenide," Nano Lett. **21**, 7602–7608 (2021).

[25] D. B. Sulas-Kern, H. Zhang, Z. Li, and J. L. Blackburn, "Microsecond charge separation at heterojunctions between transition metal dichalcogenide monolayers and single-walled carbon nanotubes," Mater. Horiz. **6**, 2103–2111 (2019).

[26] D. Sulas-Kern, H. Zhang, K. Li, and J. Blackburn, Nanoscale **13**, 8188–8198 (2021).

[27] A.-M. Dowgiallo, K. Mistry, J. Johnson, and J. Blackburn, ACS Nano **8**, 8573–8581 (2014).

[28] A. R. Myers, Z. Li, M. K. Gish, J. D. Earley, J. C. Johnson, M. A. Hermosilla-Palacios, and J. L. Blackburn, "Ultrafast charge transfer cascade in a mixed-dimensionality nanoscale trilayer," ACS Nano **18**, 8190–8198 (2024).

[29] J. Kim, C. Jin, B. Chen, H. Cai, T. Zhao, P. Lee, S. Kahn, K. Watanabe, T. Taniguchi, S. Tongay *et al.*, "Observation of ultralong valley lifetime in WSe₂/MoS₂ heterostructures," Sci. Adv. **3**, e1700518 (2017).

[30] Z. Qiu, M. Trushin, H. Fang, I. Verzhbitskiy, S. Gao, E. Laksono, M. Yang, P. Lyu, J. Li, S. Su, M. Telychko, K. Watanabe, T. Taniguchi, J. Wu, A. H. C. Neto, L. Yang, G. Eda, S. Adam, and J. Lu, "Giant gate-tunable bandgap renormalization and excitonic effects in a 2D semiconductor," Sci. Adv. **5**, eaaw2347 (2019).

[31] A. V. Stier, N. P. Wilson, G. Clark, X. Xu, and S. A. Crooker, "Probing the influence of dielectric environment on excitons in monolayer WSe₂: Insight from high magnetic fields," Nano Lett. **16**, 7054–7060 (2016).

[32] J. Fontanella, C. Andeen, and D. Schuele, "Low-frequency dielectric constants of α-quartz, sapphire, MgF₂, and MgO," J. Appl. Phys. **45**, 2852–2854 (1974).

[33] A. K. Harman, S. Ninomiya, and S. Adachi, "Optical constants of sapphire (α-Al₂O₃) single crystals," J. Appl. Phys. **76**, 8032–8036 (1994).

[34] V. Perebeinos, J. Tersoff, and P. Avouris, "Scaling of excitons in carbon nanotubes," Phys. Rev. Lett. **92**, 257402 (2004).

[35] Y. Miyauchi, R. Saito, K. Sato, Y. Ohno, S. Iwasaki, T. Mizutani, J. Jiang, and S. Maruyama, "Dependence of exciton transition energy of single-walled carbon nanotubes on surrounding dielectric materials," Chem. Phys. Lett. **442**, 394–399 (2007).

[36] K. Eckstein and T. Hertel, "Electronic structure and scaling of Coulomb defects in carbon nanotubes from modified Hückel calculations," J. Phys. Chem. C **127**, 23760–23767 (2023).

[37] T. Nishihara, A. Takakura, M. Shimasaki, K. Matsuda, T. Tanaka, H. Kataura, and Y. Miyauchi, "Empirical formulation of broadband complex refractive index spectra of single-chirality carbon nanotube assembly," Nanophotonics **11**, 1011–1020 (2022).

[38] J. M. Siqueiros, R. Machorro, and L. E. Regalado, "Determination of the optical constants of MgF₂ and ZnS from spectrophotometric measurements and the classical oscillator method," Appl. Opt. **27**, 2549–2553 (1988).

[39] A. Faridi, D. Culcer, and R. Asgari, "Quasiparticle band-gap renormalization in doped monolayer MoS₂," Phys. Rev. B **104**, 085432 (2021).

[40] R. Almaraz, T. Sayer, J. Toole, R. Austin, Y. Farah, N. Trainor, J. M. Redwing, A. Krummel, A. Montoya-Castillo, and J. Sambur, "Quantifying interfacial energetics

of 2D semiconductor electrodes using in situ spectroelectrochemistry and many-body theory," Energy Environ. Sci. **16**, 4522–4529 (2023).

[41] G. M. Carroll, H. Zhang, J. R. Dunklin, E. M. Miller, N. R. Neale, and J. Van De Lagemaat, "Unique interfacial thermodynamics of few-layer 2D MoS$_2$ for (photo)electrochemical catalysis," Energy Environ. Sci. **12**, 1648–1656 (2019).

[42] K. Yao, A. Yan, S. Kahn, A. Suslu, Y. Liang, E. Barnard, S. Tongday, A. Zettl, N. Borys, and P. J. Schuck, "Optically discriminating carrier-induced quasiparticle band gap and exciton energy renormalization in monolayer MoS$_2$," Phys. Rev. Lett. **119**, 087401 (2017).

[43] J. Pak, I. Lee, K. Cho, J.-K. Kim, H. Jeong, W.-T. Hwang, G. H. Ahn, K. Kang, W. J. Yu, A. Javey et al., "Intrinsic optoelectronic characteristics of MoS$_2$ photo-transistors via a fully transparent van der Waals heterostructure," ACS Nano **13**, 9638–9646 (2019).

[44] K. F. Mak, K. He, C. Lee, G. H. Lee, J. Hone, T. F. Heinz, and J. Shan, "Tightly bound trions in monolayer MoS$_2$," Nat. Mater. **12**, 207–211 (2013).

[45] K. P. Dhakal, D. L. Duong, J. Lee, H. Nam, M. Kim, M. Kan, Y. H. Lee, and J. Kim, "Confocal absorption spectral imaging of MoS$_2$: Optical transitions depending on the atomic thickness of intrinsic and chemically doped MoS$_2$," Nanoscale **6**, 13028–13035 (2014).

14 August 2024 15:20:19